

REPORT No. 636

APPROXIMATE STRESS ANALYSIS OF MULTISTRINGER BEAMS WITH SHEAR DEFORMATION OF THE FLANGES

By PAUL KUHN

SUMMARY

The problem of skin-stringer combinations used as axially loaded panels or as covers for box beams is considered from the point of view of the practical stress analyst. By a simple substitution the problem is reduced to the problem of the single-stringer structure, which has been treated in N. A. C. A. Report No. 608. The method of making this substitution is essentially empirical; in order to justify it, comparisons are shown between calculations and strain-gage tests of three beams tested by the author and of one compression panel and three beams tested and reported elsewhere.

INTRODUCTION

A combination of a plate and stringers is frequently used as a structural element. Figure 1 (a) shows such a combination used as a tension member; figure 1 (b) shows one used as the tension side of a beam. The stress distribution in structures of this type is materially influenced by the shear deformation of the plate. In aeronautical structures, where the plate often consists of a thin sheet that may be allowed to buckle into a diagonal-tension field, it becomes necessary to consider the effect of this shear deformation more carefully than is customary in other types of structure.

Reference 1 discusses in detail the fundamental principles and the simplifying assumptions that permit a mathematical approach to the solution of the problem.

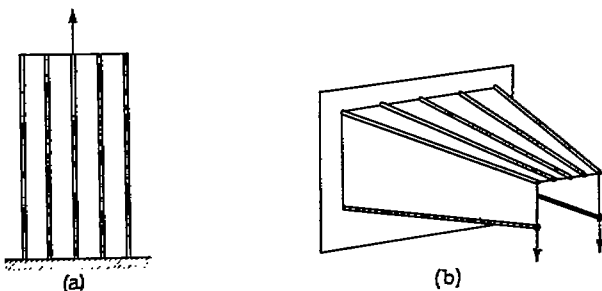


FIGURE 1.—Skin-stringer combinations as structural elements.

It is shown that numerical solutions can be obtained if there is only a single central stringer (fig. 2). A thorough familiarity with the method of analyzing single-stringer structures as given therein is presupposed. For multistringer structures the mathematics becomes so complex that there is very slight possibility of obtaining sufficiently general solutions on the basis

of the assumptions that were used for the single stringer structures.

Methods combining a desirable degree of accuracy with a reasonable degree of generality will, in all

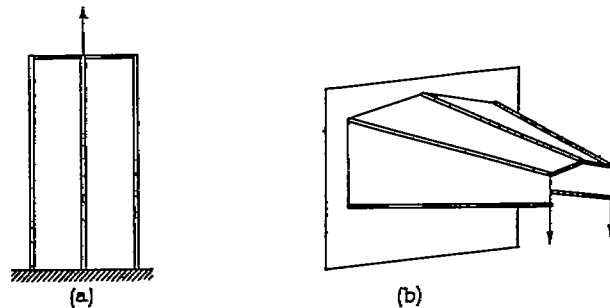


FIGURE 2.—Single-stringer structures.

probability, be methods of successive approximation. Attempts to develop such a method have thus far failed because the convergence is prohibitively slow. When such a method is found, it is not likely to be very rapid. Approximate methods developed in the interim, such as the one to be presented in this paper, will therefore retain their value by furnishing a very useful first approximation.

The method presented herein was devised to answer the urgent need for estimating the effects of shear deformation. It aims chiefly at rapidity and ease of application, which are achieved at the expense of introducing some empiricism. The experimental evidence presented is believed to be sufficient to prove that the method depicts reasonably well the influence of the shear deformation on the stringer stresses.

METHOD OF ANALYSIS

It is customary to designate tensile stresses and forces as positive. Figures, derivations, and formulas presented herein deal, in general, with tension members. The only differences between tension members and compression members are quantitative differences in the effective widths and in the effective shearing stiffnesses of the sheet. In the case of beams, the side not under consideration at the moment, i. e., the compression side in most of the discussion of this paper, is assumed to be concentrated at the shear web (figs. 1 (b) and 2 (b)) in such a location that the effective depth is not changed.

The investigation of reference 1 was restricted to symmetrical structures as indicated in figures 1 and 2. The same restriction will be made in the present paper, and formulas and numerical data must be understood to apply to the half structure unless otherwise specified.

In order to unify the terminology, the designations and symbols used in reference 1 for beams are extended in the present paper to axially loaded panels. (See appendix A for a list of symbols.) The directly loaded stringer of an axially loaded panel will therefore be referred to as the "flange" (subscript F) and the other stringers attached to the sheet as "longitudinals" or "stringers" (subscript L). This procedure is justified because the axially loaded panel may be considered as the cover of a box beam in pure bending under the assumptions made.

It is assumed in all cases that the longitudinals are distributed uniformly along the chord. It is furthermore assumed that camber is moderate, not exceeding the amounts found, for instance, in wing beams. Finally, it is assumed that the effective shear stiffness and the sheet thickness are constant along the chord.

GENERAL PRINCIPLES OF METHOD OF ANALYSIS

The mathematics of the multistring beam with variable cross section is too complex to admit of ready solution. Broadly speaking, two methods of procedure may be used in such a case. One method would be to use approximate methods of solving the equations; the other method would be to idealize and simplify the physical concept of the structure until the mathematical relations become manageable. The second method is used in this paper.

The results obtained in reference 1 show that the highest stresses occur at the flange and that they decrease from the flange toward the center line of the structure. The stress in the flange and the closely related stress in the longitudinal adjacent to the flange are therefore of paramount interest to the analyst.

In beams with cambered cover, which were not treated in reference 1, the highest stress in the longitudinals may occur adjacent to the flange or it may occur at the center line of the beam. When it occurs at the center line, the stress there also becomes a matter of concern to the analyst.

It is quite obvious that, in general, the most important physical actions will take place around the flanges, partly because the loads are applied there and partly because the stresses reach a maximum there as long as there is no violation of the basic requirement that the camber be very moderate. Consequently, any simplification that may be made should affect as little as possible the picture of the physical relations in the immediate vicinity of the flanges.

In conformance with this requirement, the simplification necessary for obtaining a solution was achieved by using a "substitute structure" obtained by leaving the

flange (and shear web) intact but replacing the longitudinals that are actually uniformly distributed over the width of the sheet by a single longitudinal equivalent to them as far as action on the flange is concerned. This substitution reduces the problem of the multistringer structure to that of the single-stringer structure, which can be analyzed as shown in reference 1. The method of substituting (temporarily) a simplified structure for the actual one corresponds in part to the method of using "phantom members" in trusses.

The substitute structure is used only to calculate the stresses in the part that it has in common with the actual structure, namely, the flange and the skin adjacent to the flange. After this object has been attained, the substitute structure is discarded. The stresses in the actual distributed longitudinals are then obtained by using the method described in reference 1 for distributing "corrected forces."

It is clear that, in any given case, at least one equivalent single longitudinal exists. Whether or not there is a general method for finding this equivalent longitudinal, however, is a question that could be answered theoretically only if all the exact mathematical solutions were known. They are not known, and the method of finding the equivalent longitudinal is therefore essentially empirical and must be justified by tests. This requirement is not such a serious drawback as it may seem to be, because the basic simplifications used are such that experimental verification is required in any event.

The method of finding the equivalent single longitudinal is as follows: Remove from the sheet each individual stringer of cross-sectional area A at a distance y from the center line and attach, at the center line of the structure, a substitute stringer with a cross-sectional area

$$A_s = A \frac{\sigma_y}{\sigma_{CL}} \quad (1)$$

where σ_y is the stress in the actual stringer and σ_{CL} the stress in the actual center-line stringer. The ratio σ_y/σ_{CL} may be considered as the "effectiveness" of the stringer at y relative to the stringer at the center line $y=0$; the use of this factor in expression (1) tends to counteract the loss of effectiveness caused by moving the stringer from its original location to the center line. The sum of the individual substitute stringers attached at the center line constitutes the single equivalent longitudinal.

As the stresses σ_y and σ_{CL} are unknown at the outset, for a first approximation, the ratio σ_y/σ_{CL} is obtained from equation (17) of the constant-stress solution given in reference 1. With the stresses thus computed, a second approximation might be made. In all cases investigated thus far, it was found that the second approximation agreed with the first one within the limits of experimental accuracy. The use of the second approximation is therefore considered unnecessary. (It must

be borne in mind that the method of finding the equivalent longitudinal is essentially empirical. Consequently, there is no valid reason to believe that the second approximation must be better than the first one.)

ANALYSIS OF AXIALLY LOADED PANEL

As an example of the analysis of an axially loaded panel, the analysis of the compression panel with seven stiffeners, described in reference 2, will be discussed in detail. The pertinent data on this panel are given in figures 3 (a) and 3 (b).

Estimate of effective areas and of effective shear stiffness.—The test results are given in reference 2 for $2P=2,000, 4,000,$ and $6,000$ pounds. The analysis will be made for $2P=4,000$ or $P=2,000$ pounds. It will become apparent that the conditions at this load are the same as for very small loads, so that the analysis will be valid for any load between 0 and 4,000 pounds.

The mean stress in the panel (reference 2) is

$$\sigma_M = \frac{2,000}{0.70} = 2,860 \text{ lb./sq. in.}$$

This stress is fairly close to the compressive buckling stress of the sheet; the effective width of the sheet will therefore be taken as equal to the actual width. The effective stringer area for the flange is therefore

$$A_F = 0.180 + 2 \times 0.024 = 0.228 \text{ sq. in.}$$

and for the sum of the other stringers

$$A_L = 2.5 \times 0.088 + 10 \times 0.024 = 0.460 \text{ sq. in.}$$

The force at the bottom of the edge stringer is approximately

$$F_F = 2,860 \times 0.228 = 652 \text{ lb.}$$

leaving 1,348 pounds to be transmitted by shear in the sheet to the other stringers. The average shear stress in the sheet next to the edge stringer is therefore

$$\tau = \frac{1,348}{48 \times 0.024} = 1,170 \text{ lb./sq. in.}$$

The critical buckling stress for 0.024-inch dural sheet, 4 inches wide and assumed simply supported, is, according to Timoshenko,

$$\tau_{crit} = 1,730 \text{ lb./sq. in.}$$

This value is so far above the actual stress that there is no possibility of a diagonal-tension field forming and reducing the shear stiffness, so that $G_s/E=0.40$ may be taken.

Determination of substitute structure.—Figure 3 (c) shows the cross section of the idealized structure

assumed for the analysis. The stringer areas given on this figure are effective areas that include the effective width of the sheet; the sheet is now assumed to carry only shear.

If there are at least two intermediate stringers between the center stringer and the flange, the calculation of the substitute stringer may be simplified by using a formula derived on the assumption that there are infinitely many intermediate stringers; that is, on the

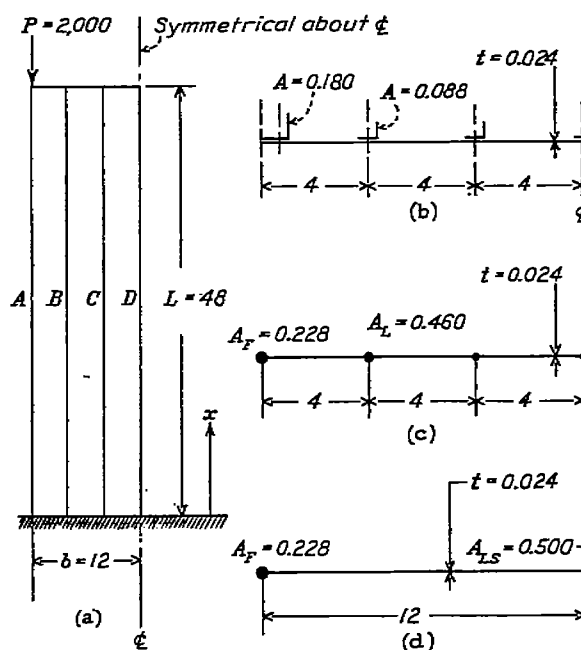


FIGURE 3.—Compression panel used for sample analysis.

assumption that the area A_L of the intermediate stringers is distributed uniformly along the width b of the sheet. The derivation of this formula is as follows: According to the constant-stress solution (reference 1, equation (17))

$$\frac{\sigma_y}{\sigma_{cz}} = \cosh K_3 y \tag{2}$$

where

$$K_3 y = K_3 b \times \frac{y}{b}$$

and, in the case of a constant cross section,

$$K_3 b = \sqrt{\frac{A_L b E}{t L^2 G_s}} \tag{3}$$

The area of an individual stringer is now

$$dA_L = \frac{A_L}{b} dy$$

and the area of the substitute stringer that replaces it at the center line is, according to equation (1),

$$dA_{LS} = \frac{A_L}{b} dy \cosh K_3 y$$

The total area of the substitute stringer located at the center line is therefore

$$A_{LS} = \frac{A_L}{b} \int_0^b \cosh K_3 y \, dy = A_L \frac{\sinh K_3 b}{K_3 b} \quad (4)$$

In the case under consideration

$$K_3 b = \sqrt{\frac{2 \times 0.460 \times 12}{0.024 \times 48^2 \times 0.40}} = 0.706$$

so that

$$A_{LS} = 0.460 \times \frac{0.767}{0.706} = 0.500 \text{ sq. in.}$$

Figure 3 (d) shows the cross section of the substitute structure.

Analysis of substitute structure.—The substitute structure of figure 3 (d) can be analyzed by applying the formulas given in appendix B. By formula (A-1)

$$K^2 = \frac{0.40 \times 0.024}{12} \left(\frac{1}{0.228} + \frac{1}{0.500} \right)$$

$$K = 0.0715$$

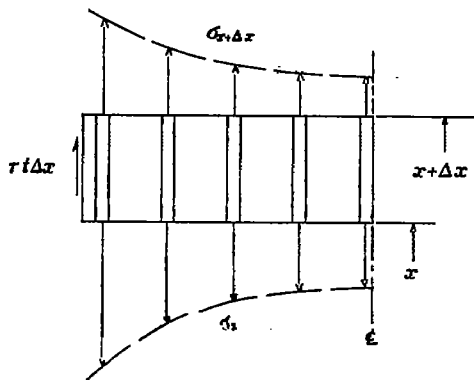


FIGURE 4.—Free-body diagram for calculating shear stress.

For any station along the span, the stresses and forces can now be calculated. For example, at the bottom of the panel ($x=0$), by formula (A-3)

$$\begin{aligned} \sigma_F &= \frac{P}{A_F + A_{LS}} \left(1 + \frac{A_{LS}}{A_F} \frac{\cosh Kx}{\cosh KL} \right) \\ &= \frac{2,000}{0.228 + 0.500} \left(1 + \frac{0.500 \times 1.00}{0.228 \times 15.53} \right) \\ &= 3,134 \text{ lb./sq. in.} \end{aligned}$$

With the computation of σ_F the substitute structure has served its purpose and is discarded. It is important not to confuse it with the actual structure in any of the following computations.

Calculation of stresses in longitudinals.—The total force F_L in the actual longitudinals is

$$F_L = P - F_F = P - \sigma_F A_F$$

or, at $x=0$,

$$F_L = 2,000 - 3,134 \times 0.228 = 1,286 \text{ lb.}$$

This force is to be distributed over the longitudinals by the method given in reference 1, equations (21) and

(22).—In order to apply this method, compute the average stress

$$\sigma_{L_{av}} = \frac{F_L}{A_L} = \frac{1,286}{0.460} = 2,800 \text{ lb./sq. in.}$$

and the ratio

$$\frac{\sigma_{L_{av}}}{\sigma_F} = \frac{2,800}{3,134} = 0.894$$

With this ratio as abscissa, read from figure 18 of reference 1 (redrawn to a larger scale)

$$Yb = 0.605$$

and calculate

$$\sigma_{CL} = \frac{\sigma_F}{\cosh Yb} = \frac{3,134}{1.188} = 2,640 \text{ lb./sq. in.}$$

For the other two stringers, which are located at $y = \frac{1}{2}b$ and $y = \frac{3}{2}b$, the stress will be, for stringer C,

$$\sigma = \sigma_{CL} \cosh Yy = 2,640 \times \cosh 0.202 = 2,694 \text{ lb./sq. in.}$$

and, for stringer B,

$$\sigma = 2,640 \times \cosh 0.404 = 2,860 \text{ lb./sq. in.}$$

The shear stress τ at any point in the sheet is obtained most conveniently by considering the equilibrium of an element Δx cut out of the structure as indicated in figure 4, taking advantage of the fact that the shear stress is zero at the center line. The shear stress in the first panel next to the flange, which is the most important one for design purposes, will be obtained automatically as part of the solution of the substitute structure if the numerical trial-and-error method of solution is used, or by using formula (A-2) from appendix B in the case of a constant-section panel.

Panels with variable cross section.—In the case of a panel with variable cross section, the panel is divided into a convenient number of bays as described in reference 1. For each bay, the cross-sectional area of the substitute longitudinal is computed by using formula (4). In the computation of $K_3 b$ by formula (3), the average values in the bay are used for A_L , b , t , and G_d/E . The length L is again the total length of the panel (not of the bay). The analysis of the substitute structure is made by the trial-and-error method described in reference 1. After this step, the procedure is identical with the procedure for constant-section panels.

ANALYSIS OF BEAMS WITH FLAT COVERS

The analysis of beams with flat covers is so closely analogous to the analysis of axially loaded panels that no detailed example need be given. The substitute structure is found exactly as for an axially loaded panel. The resulting beam with a single longitudinal is analyzed by the trial-and-error method described in reference 1, or by formulas if applicable. The total force F_L at any section can then be distributed over the longitudinals as previously described.

ANALYSIS OF BEAMS WITH CAMBERED COVERS

The cambered beam with a single longitudinal.—The basic problem of the beam with a single longitudinal and a cambered cover was not treated in reference 1. It will now be briefly discussed.

Figure 5 shows an element of length dx cut out of the beam. With the help of this diagram, the fundamental equations of equilibrium can be written exactly as in the case of the beam with a flat cover (reference 1, equations (3a) and (3b) ¹).

$$dF_F = S_w \frac{dx}{h_w} - dS_C \tag{5a}$$

$$dF_L = dS_C \tag{5b}$$

The equation that expresses the relation between shear stress and longitudinal stresses is slightly more complicated than in the case of a flat cover. The ordinary bending theory may be taken to give the limiting case of no shear deformation. The deformations that determine the shear strain must therefore be measured from the plane cross section of the engineering bending theory as a reference base, resulting in the equation

$$d\tau = -\frac{G_s}{E\bar{U}}[(\sigma_F - \sigma_{FP}) - (\sigma_L - \sigma_{LP})]dx \tag{5c}$$

where the subscript P denotes stresses obtained with the engineering bending theory, which assumes plane sections to remain plane.

These equations can be used to obtain numerical solutions by the trial-and-error method, using finite differences Δ in place of the differentials d . Appendix B gives the analytical solution for two cases that correspond to the solutions given for a beam with a flat cover in reference 1.

¹In reference 1, equation (3b) is written incorrectly with a minus sign ahead of dF_L .

The cambered beam with many longitudinals.—In the treatment of the cambered beam with many longitudinals shown in figure 6 (a), various degrees of refinement are possible. The following method, devised

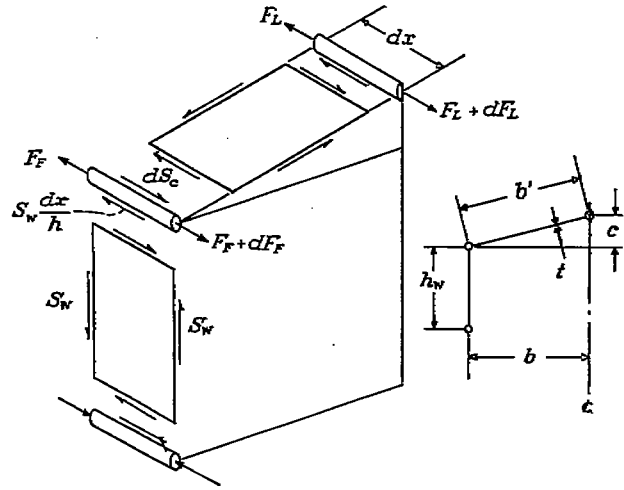


FIGURE 5.—Free-body diagrams and notation for single-stringer beam with cambered cover.

to utilize the method developed for axially loaded panels and for beams with flat covers, is believed to be adequate for practical purposes. Attention is called again to the basic assumption stated previously, i. e., that the camber is moderate.

The analysis is again divided into two steps: the calculation of the flange stresses σ_F along the span by means of the substitute structure, and the subsequent distribution of the force F_L over the longitudinals at any station.

The area of the substitute stringer is calculated by equation (4), using for b the developed width of the cover sheet. The camber of the substitute beam may, for practical purposes, be taken as $c_s = \frac{1}{2} c$ (fig. 6 (b)).

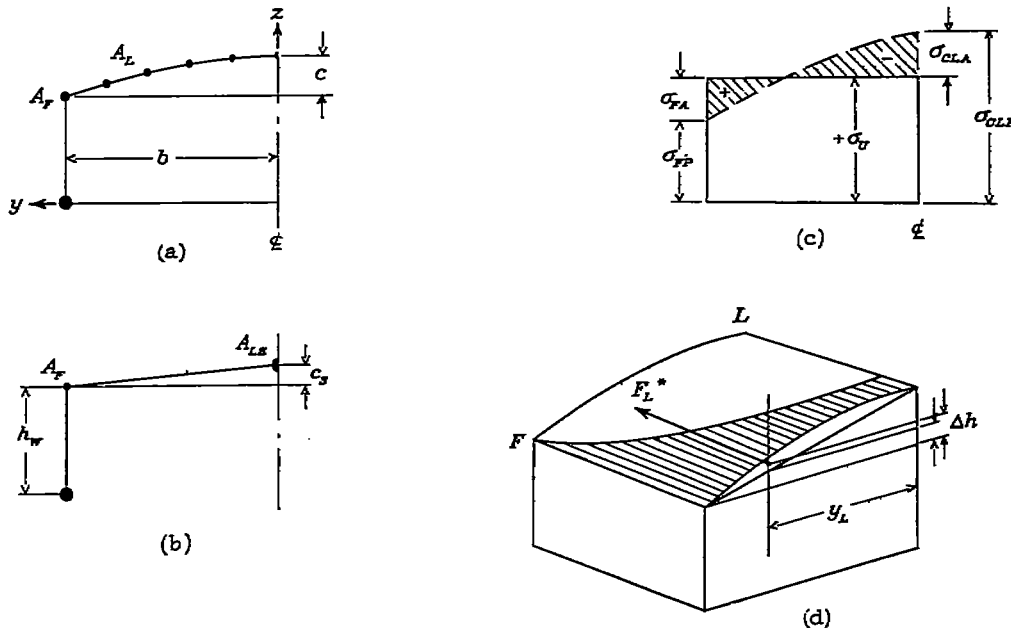


FIGURE 6.—Cambered-cover beam.

The distribution of the force F_L cannot be made directly by the method used for flat panels. In the flat panel, the longitudinal stress is uniform along the chord in the limiting case of infinite shear stiffness; in the case of finite shear stiffness, the shear strain is defined directly by the longitudinal strains. In the cambered cover with infinite shear stiffness, the stress varies along the chord according to the straight-line law of the ordinary bending theory; in the cambered cover with finite shear stiffness, the shear strains are defined by the differences between the longitudinal strains and the corresponding strains of the ordinary bending theory as indicated by equation (5c).

These differences between the cambered and the flat cover may be interpreted as arising from the fact that the cambered cover has bending stiffness of its own because it has a "beam depth" equal to its camber.

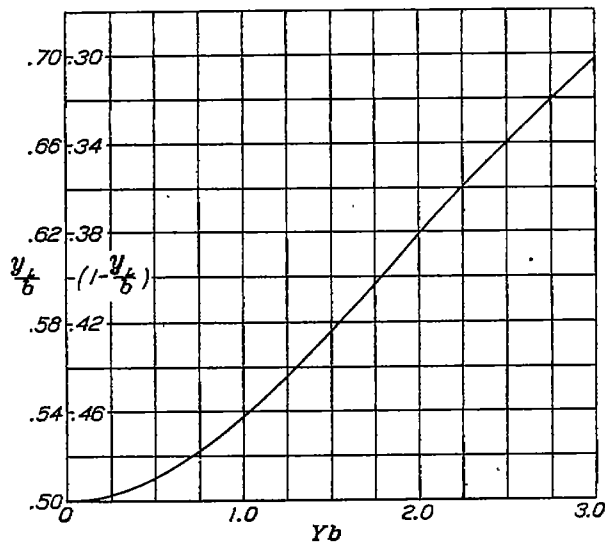


FIGURE 7.—Graph for location of resultant force on cover.

In the single-stringer beam it was not difficult to take care of the effect of this bending stiffness mathematically by introducing the terms σ_{FP} and σ_{LP} into equation (5c). In the multistring beam it is more convenient to introduce a physical equivalent, namely, an auxiliary system of longitudinal stresses distributed over the cover in such a manner as to make the stress uniform in the limiting case of infinite shear stiffness. In figure 6 (c) the broken line shows the stresses given by the ordinary bending theory, the full line shows the uniform stress, denoted by σ_U , and the cross-hatched area between the two lines indicates the auxiliary stresses necessary to achieve the uniform stress distribution. The magnitude of the uniform stress is determined by the condition that, when the auxiliary stresses act on the flange A_F and on the longitudinals A_L , they must not change the bending moment acting at the section, i. e., they must have zero moment about the assumed centroidal line of the lower cover. The auxiliary stresses will be denoted by a second subscript A placed

after the first subscript, which denotes the stringer or flange where the stress is measured.

With the auxiliary stresses assumed active, the method of finding the distribution of the stresses along the chord is analogous to the method used for flat panels and will be shown in detail for a numerical example. From the stresses thus calculated, the auxiliary stresses are subtracted to obtain the final stresses.

One step not necessary in the analysis of flat panels is required for cambered covers. As indicated in figure 6 (d), it is necessary to locate the resultant force F_L^* acting on the cover (exclusive of the flange) when the actual and the auxiliary stresses are acting. The vertical location Δh of this resultant determines the effective depth of the beam

$$h_e = h_W + \Delta h \quad (6)$$

when the combined stresses are acting. The exact calculation of Δh would require a very tedious integration involving the stress distribution and the shape of the cover, which has to be repeated several times for each cross section with slightly differing values of stress distribution. For practical purposes, it will therefore be advisable to simplify the problem, although there will be a slight loss in accuracy, by finding the lateral location y_L of the resultant and by assuming that Δh is determined by the intersection of the line $y = y_L$ and the straight line joining F and L , as indicated in figure 6 (d). Under the assumption of moderate camber, y_L is given by

$$\begin{aligned} y_L &= \frac{\int_0^b \sigma^* y dA}{\int_0^b \sigma^* dA} \\ &= \frac{1}{Y} (Yb - \coth Yb + \operatorname{csch} Yb) \end{aligned}$$

where Y is the parameter introduced in reference 1, equation (21), for the purpose of distributing stresses chordwise. The value of y_L/b is plotted in figure 7 against Yb for ready reference. With the proposed simplification, the value of Δh is then given by

$$\Delta h = c(1 - y_L/b) \quad (7)$$

NUMERICAL EXAMPLE FOR ANALYSIS OF A CAMBERED BEAM

Figure 8 (a) shows the cross section of the beam assumed for the sample analysis. The root section will be analyzed for a load P of 250 pounds acting at the tip; the length L of the beam is 108 inches. It is assumed that the effective width of the sheet has been estimated and that the value $A_L = 0.85$ sq. in. includes the effective width.

The next step is to estimate the effective shear modulus. If the presence of camber and of shear deformation is neglected, the maximum shear stress in the sheet will be given by formula (A-8) of appendix B as

$$\tau_{max} = \frac{PA_L}{t h A_T} = \frac{250 \times 0.85}{0.0115 \times 3 \times 1.65} = 3,730 \text{ lb./sq. in.}$$

The buckling shear stress of a long dural plate 0.0115 inch thick and 1.80 inches wide is

$$\tau_{crit} = 1,960 \text{ lb./sq. in.}$$

The maximum shear stress being only about twice the critical stress, the average shear stress is sufficiently close to the critical to neglect diagonal-tension effects on shear stiffness and to set $G_s = G$ or $G_d/E = 0.40$.

Equation (3) then gives

$$K_3 b = \sqrt{\frac{2 \times 0.85 \times 9}{0.0115 \times 108^2 \times 0.40}} = 0.535$$

Inserting this value in equation (4) gives

$$A_{LS} = 0.85 \frac{0.561}{0.535} = 0.892 \text{ sq in.}$$

The cross section of the substitute beam is shown in figure 8 (b). Since the substitute beam is of uniform cross section, it can be solved analytically. Formula (A-14) gives

$$K^2 = \frac{0.40 \times 0.0115}{9} \left(\frac{1 + \frac{1}{3}}{0.80} + \frac{1}{0.892} \right)$$

$$K = 0.0378 \quad KL = 4.08$$

Formula (A-12) then gives for $x = 108$ inches

$$\sigma_F = \frac{27,000 \times 0.94}{9.20} \left[1 + \frac{1.94 \times 0.892}{0.94 \times 0.80} \left(1 + \frac{1}{3} \right) \frac{0.999}{4.08} \right]$$

$$\sigma_F = 4,830 \text{ lb./sq. in.}$$

This computation completes the first step and the substitute beam is discarded.

The next step is to calculate the stresses in the actual beam by the ordinary bending theory:

$$\sigma_{FP} = \frac{27,000 \times 0.94}{9.65} = 2,630 \text{ lb./sq. in.}$$

$$\sigma_{CLP} = \frac{27,000 \times 2.94}{9.65} = 8,220 \text{ lb./sq. in.}$$

Figure 8 (c) shows the chordwise distribution of the stresses according to the ordinary bending theory as well as the auxiliary stresses. In order to show that the auxiliary stresses indicated by figure 8 (c) fulfill the requirements, a check on their total moment is made.

$$\begin{aligned} 1,955 \times 3 \times 0.80 &= 4,690 \\ 837 \times 3.4 \times 0.189 &= 538 \\ -281 \times 3.8 \times 0.189 &= -202 \\ -1,399 \times 4.2 \times 0.189 &= -1,111 \\ -2,517 \times 4.6 \times 0.189 &= -2,188 \\ -3,635 \times 5.0 \times 0.0945 &= -1,717 \end{aligned}$$

The moment is zero with a negligible error. The flange stress used for calculating the chordwise stress distribution is therefore

$$\sigma_F^* = \sigma_F + \sigma_{FA} = 4,830 + 1,955 = 6,785 \text{ lb./sq. in.}$$

The moment furnished by the flange is

$$M_F^* = 6,785 \times 0.80 \times 3.00 = 16,280 \text{ in.-lb.}$$

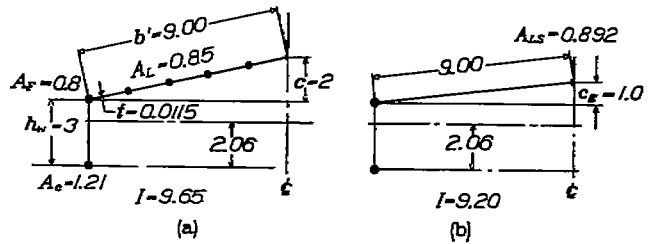


FIGURE 8.—Cambered-cover beam for sample analysis.

The moment to be furnished by the cover longitudinals is therefore

$$M_L^* = 27,000 - 16,280 = 10,720 \text{ in.-lb.}$$

Assuming $h_c = 3.77$ inches, the force F_L^* becomes

$$F_L^* = \frac{10,720}{3.77} = 2,840 \text{ lb.}$$

The average stress is therefore

$$\sigma_{L_{av}}^* = \frac{2,840}{0.85} = 3,345$$

and the ratio

$$\frac{\sigma_{L_{av}}^*}{\sigma_F^*} = \frac{3,345}{6,785} = 0.493$$

With this value as abscissa, read from figure 18 of reference 1

$$Yb = 1.94$$

and, with this value,

$$y_L/b = 0.613$$

from figure 7 so that

$$\Delta h = 2(1 - 0.613) = 0.77 \text{ in.}$$

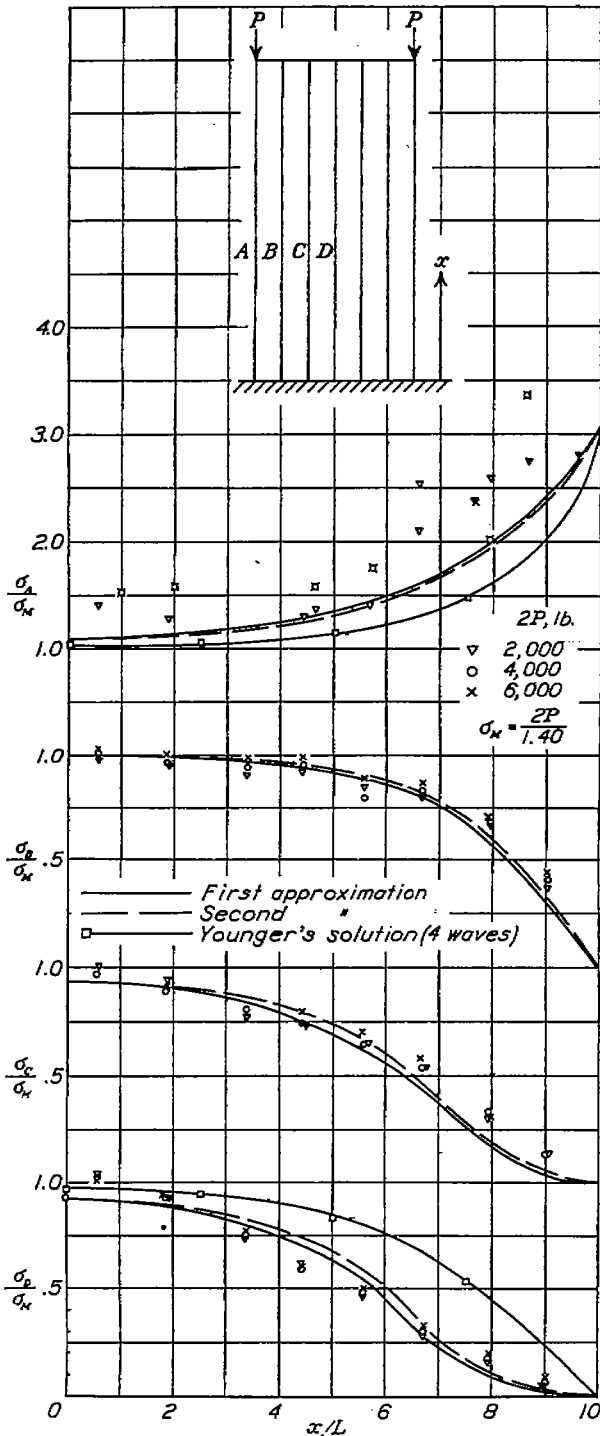


FIGURE 9.—Stresses in axially loaded panel (experimental data from reference 2).

and

$$h_e = 3.00 + 0.77 = 3.77 \text{ in.}$$

which agrees with the assumed value. If it did not agree, a new trial would have to be made.

The stress at the center line is given by

$$\sigma_{CL}^* = \frac{\sigma_P^*}{\cosh Yb} = \frac{6,785}{3.551} = 1,910$$

From this stress the actual stress is obtained by subtracting the auxiliary stress

$$\sigma_{CL}^* = 1,910 - (-3,635) = 5,545 \text{ lb./sq. in.}$$

Table I shows the calculation of the stresses σ^* in the other stringers by the formula

$$\sigma_y^* = \sigma_{CL}^* \cosh Yy$$

and of the final stresses; figure 8 (d) shows graphically the final stress distribution.

TABLE I

Stringer	y/b	Yy	cosh Yy	(lb./sq. in.)	(lb./sq. in.)	(lb./sq. in.)
Center line	0.0	0	1.000	1,910	-3,635	5,545
1	.2	.388	1.076	2,056	-2,617	4,673
2	.4	.776	1.316	2,514	-1,399	3,913
3	.6	1.164	1.758	3,360	-261	3,641
4	.8	1.552	2.466	4,710	837	3,873
Flange	1.0	1.94	3.551	6,785	1,955	4,830

EXPERIMENTAL STUDIES

AXIALLY LOADED PANELS

Experimental results for a panel loaded in compression are described in reference 2. This panel was shown in figure 3 and served as a numerical example for the proposed method of analysis. The results of the analysis as well as the experimental results are shown in figure 9.

GENERAL REMARKS ON ANALYSIS OF BEAM TESTS

In the analysis of beam tests, some difficulty is met in establishing the idealized section. It is easy to define locations for the longitudinals but fixing the location, and particularly the size, of the flanges presents difficulties, because part of the shear web must be considered as furnishing a contribution to the idealized flange.

In order to reduce arbitrariness to a minimum, the following procedure was adopted for all beam analyses. First, the centroidal axis and the geometric moment of inertia of the cross section in question were computed. If the sheet was considered to be only partly effective in carrying normal stresses, the proper effective width was used in these computations. Next, the locations of the idealized flanges were fixed. On that side of the beam where the shear deformation was being calculated, the flange was assumed to be in the plane of the cover sheet. On the other side, which was without cover except in one case, the flange was assumed to be located at its estimated centroid. The cross-sectional areas of the two idealized flanges (tension and compression) were then computed from the conditions that the idealized section must have the same centroidal axis and the same moment of inertia as the actual section. For this idealized section, the analysis was then made by using the previously described methods.

GENERAL REMARKS ON N. A. C. A. BEAM TESTS

The available published test data were not sufficient for an adequate check of the theory developed. A number of beams were therefore tested by the N. A. C. A. The first of these beams was discussed in reference

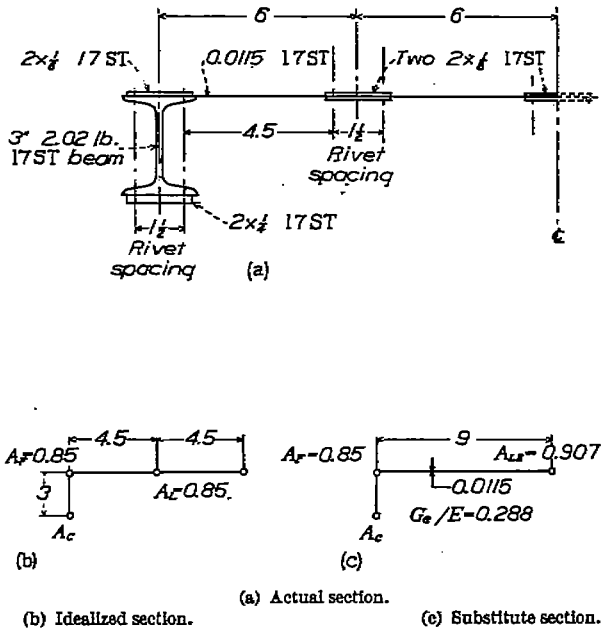


FIGURE 10.—Cross section of N. A. C. A. beam 2.

1; the following ones, designated as N. A. C. A. beams 2, 3, and 4, will be discussed in this paper.

In all N. A. C. A. beams, measurements were made on the tension side of the beam in order to eliminate

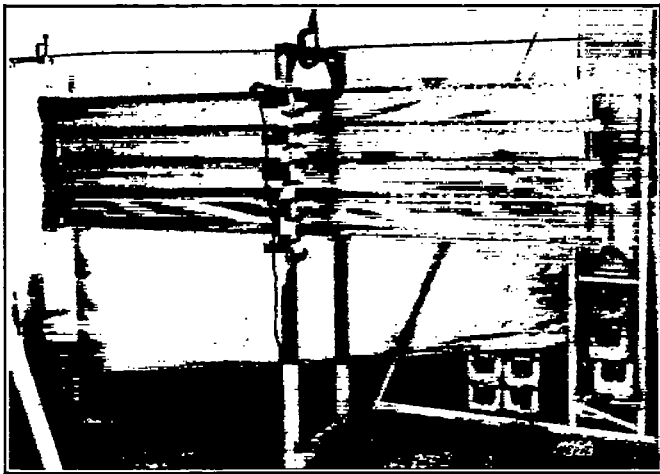


FIGURE 11.—N. A. C. A. beam 2 under test.

erroneous strain readings caused by local buckling of the stringers. Furthermore, flat strips could be used for stringers, making it possible to take strain readings very close to the sheet.

The load $2P$ was increased from 0 to 500 pounds (in the first series of tests) in steps of 50 pounds and

decreased again in steps of 100 pounds. The slope of the straight line through the test points was used to determine the stress at $P=250$ pounds, which will be shown in the later figures.

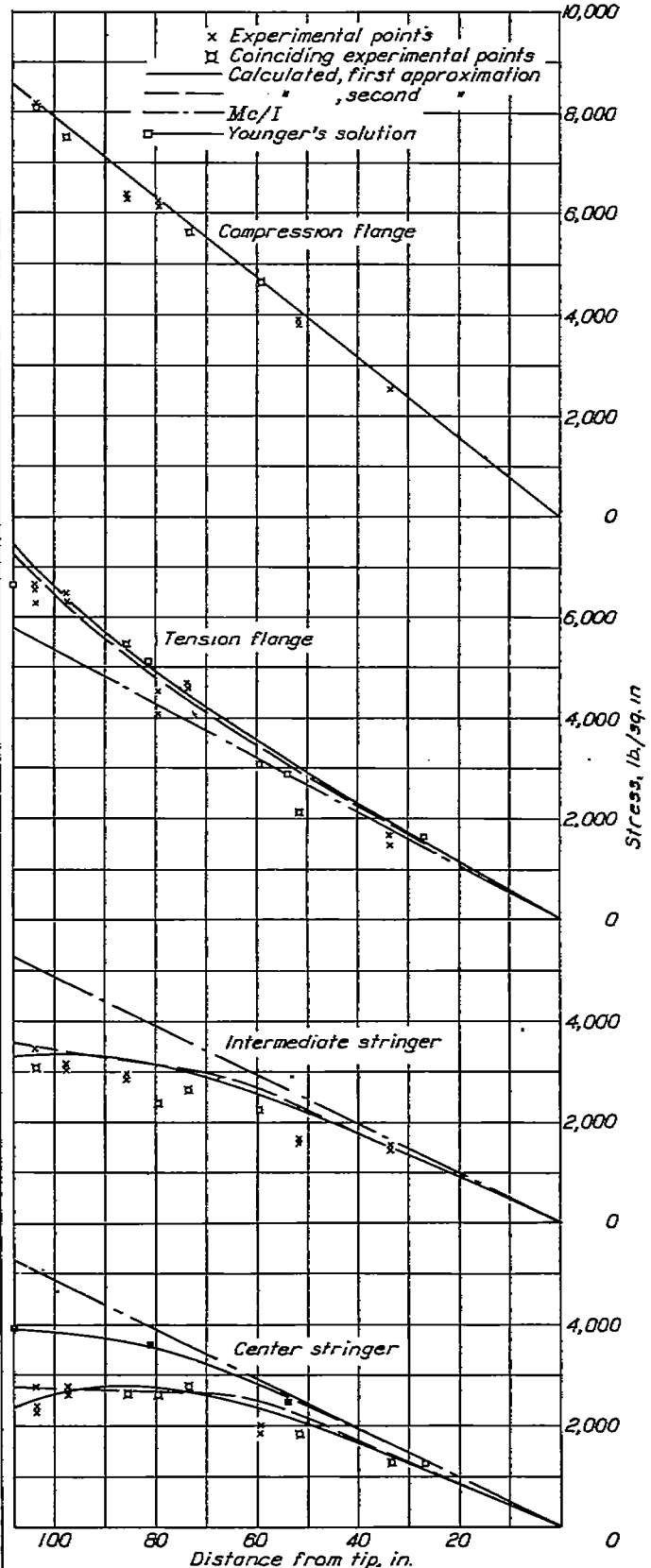


FIGURE 12.—Stresses in N. A. C. A. beam 2 for $P=250$ lb. $E=10.4 \times 10^6$.

Readings were taken across the entire section of the beam and on both sides of the stringers. Each point representing a flange stress in the figures is therefore the average of two slopes, and each point representing a stringer stress is the average of four slopes excepting figures that show the stress distribution along the entire chord.

A slight departure was made from the described method of analysis in the case of N. A. C. A. beams 2 and 3. The uniform distribution of A_z along the chord

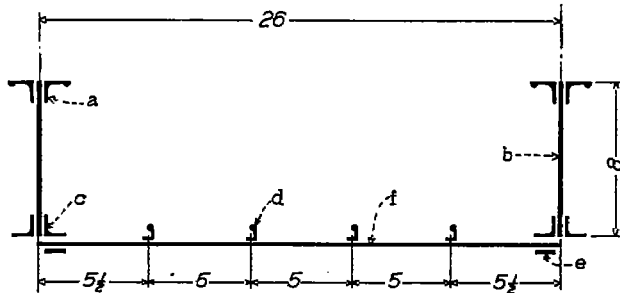


FIGURE 13.—Cross section of Galcitt beams. a, upper cap angle. Area=0.354 sq. in. b, beam web. $t=0.051$ in. c, lower cap angle. Area=0.221 sq. in. d, stiffener angle. Area=0.044 sq. in. e, attaching strip. Area=0.082 sq. in. f, cover sheet. $t_1=0.025$ in.; $t_2=0.050$ in.

is not very well approximated in these beams, A_z consisting of only two stringers. Consequently, equation (4) was not used. The two stringers constituting A_z were treated individually on the basis of equations (1) to (3). This departure also accounts for the fact that, for beam 3, the substitute camber is not taken as one-half the actual camber, as recommended for practical cases with many stringers. For comparison with the

experimental flange stresses, the stresses calculated for the idealized flanges of the N. A. C. A. beams were corrected to the outside fiber stresses on the assumption that plane sections remain plane. For the purpose of calculating the shear deformation, the width of the sheet was taken between rivet rows for N. A. C. A. beams 2 and 3.

TESTS ON BEAMS WITH FLAT COVERS

N. A. C. A. beam 2.—N. A. C. A. beam 2 was similar in design to beam 1 described in reference 1. The cross sections of the beam are shown in figure 10. The bulkheads, not shown in this figure, were similar to those on beam 1 and were spaced to make the bays about square. The length L of the beam was 108 inches. Figure 11 shows the beam under test and figure 12 shows the results of the tests and of the calculations.

Galcitt test beams.—Figure 13 shows the cross section of a type of beam tested at the California Institute of Technology (reference 3) under a pure bending moment. Figure 14 (a) shows the experimental and calculated results for the beam with $t=0.025$ inch and figure 14 (b) shows the results for the beam with $t=0.050$ inch.

Schnadel's ship model.—Figure 15 shows the cross section and the side view of a ship model tested by Schnadel (reference 4). The model was built of steel. Measurements were taken only on the outside of the compression cover (corresponding to the deck of the vessel) over one quadrant of the beam. Figure 16 shows the experimental results and the results calculated by the method presented in this paper.

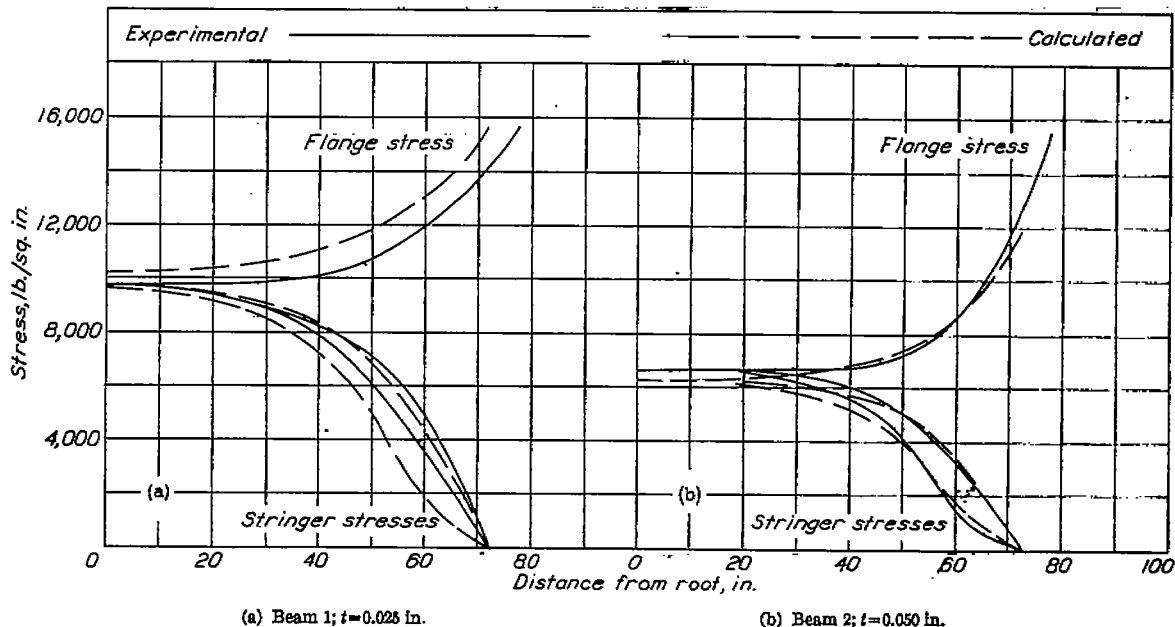


FIGURE 14.—Stress distribution in Galcitt beams. Experimental data from reference 3; $M_0=120,000$ in.-lb.; G_s/E assumed 0.25 (diagonal tension).

TESTS ON BEAMS WITH CAMBERED COVER

N. A. C. A. beam 3.—Figure 17 shows the cross sections of a cambered beam obtained by inserting cambered bulkheads into N. A. C. A. beam 2. Figure 18

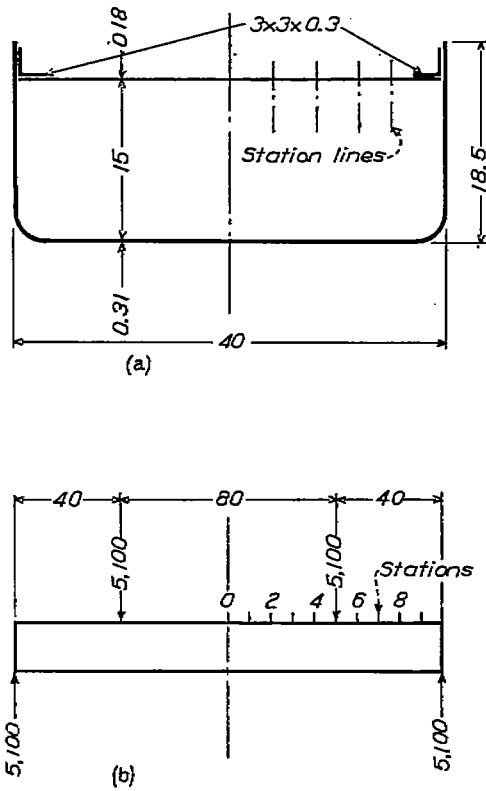


FIGURE 15.—Cross section and general diagram of Schnadel's ship model. Dimensions are in cm and loads in kg.

shows the beam under test. Figure 19 is a view of the inside of the beam, showing intermediate bulkheads that were added for tests at high loads to reduce sagging of the stringers between the main bulkheads. This sagging is proportional to the square of the stresses and consequently may become important at high

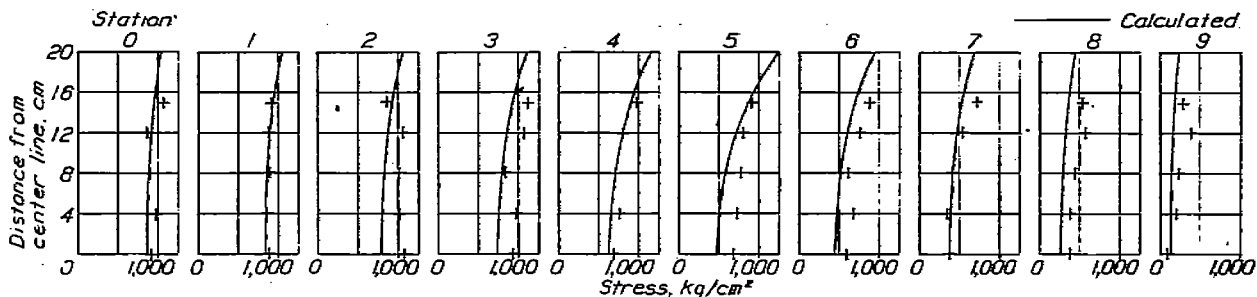


FIGURE 16.—Stress distribution in Schnadel's ship model (experimental data from reference 4).

stresses, but it requires attention only in the case of shallow beams. Figure 20 shows experimental and calculated stresses in this beam at $P=250$ pounds.

A shorter series of measurements was made on beam 3 at higher loads. Figure 21 shows the stresses at four

stations for three different loads. Two facts are evident from an inspection of this figure: The differences between the actual stresses and the stresses of the ordinary bending theory increase as the root is approached and

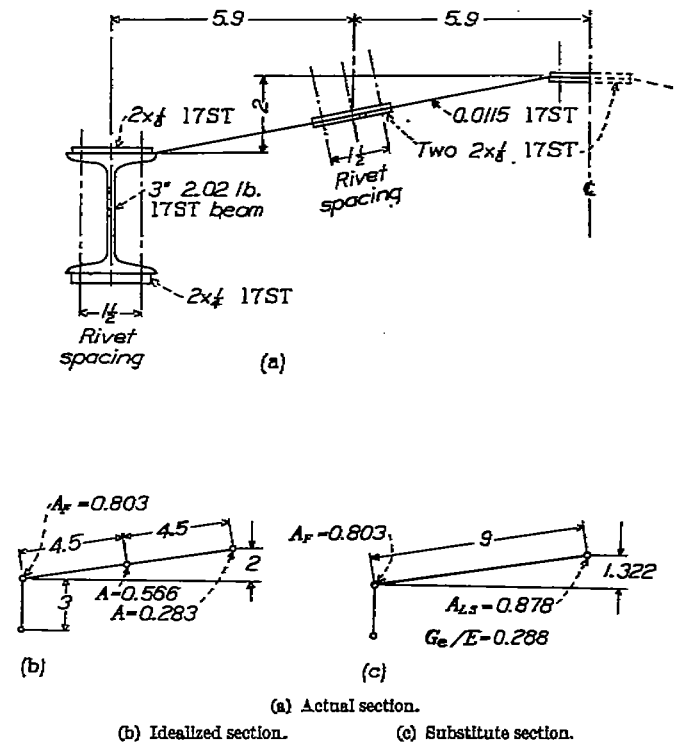


FIGURE 17.—Cross section of N. A. C. A. beam 3.

also as the load increases, because the shearing stiffness decreases with increase in load.

N. A. C. A. beam 4.—N. A. C. A. beam 4 was tapered in plan form, in depth, and in stringer area as shown in figure 22. Figure 23 shows the calculated and experimental stresses in the flange. The experimental stresses shown in this figure are based on measurements taken on the outside of the flange but are corrected to the top edge of the web.

each side. It was found that the skin stresses were consistently higher than the stringer stresses; near the root the difference was as much as 20 percent, but the difference decreased (roughly proportionally) with distance from the root. Since the ratio of stringer area to sheet area was more than 4:1, the weighted average

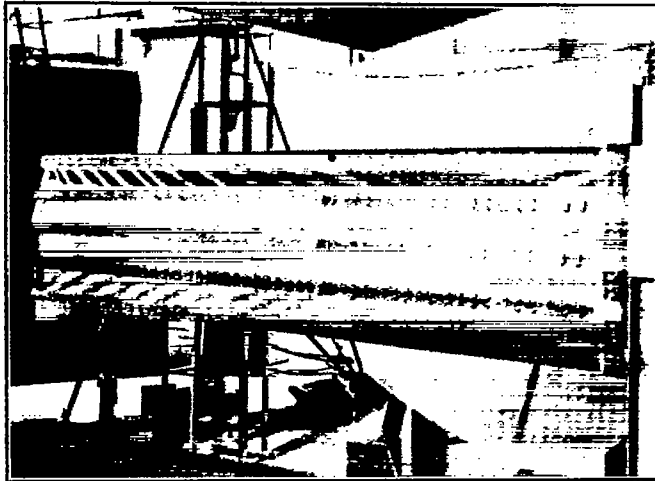


FIGURE 18.—N. A. C. A. beam 3—view of closed side.

stress never differed by more than 5 percent from the stringer stress proper.

DISCUSSION OF RESULTS

COMPARISON BETWEEN PROPOSED METHOD OF ANALYSIS AND EXPERIMENTAL RESULTS

The agreement between experiment and calculation is good for the axially loaded panel (fig. 9). For N. A.

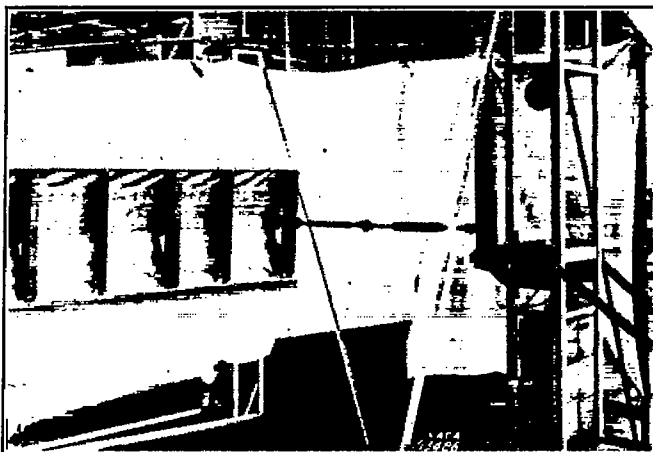


FIGURE 19.—N. A. C. A. beam 3—view of open side.

C. A. beams 2 and 3, the agreement is good except for the root region of the center stringer in beam 3 (figs. 12 and 20).

For N. A. C. A. beam 4, the agreement is reasonably good for the flange stresses (fig. 23). For the stringer stresses, which are shown only for the root station in figure 24, the agreement may be considered fair, if the differences between the two test series and the differ-

ences between stringer stresses and skin stresses, previously mentioned, are considered.

For the Galcit beams, the agreement is somewhat

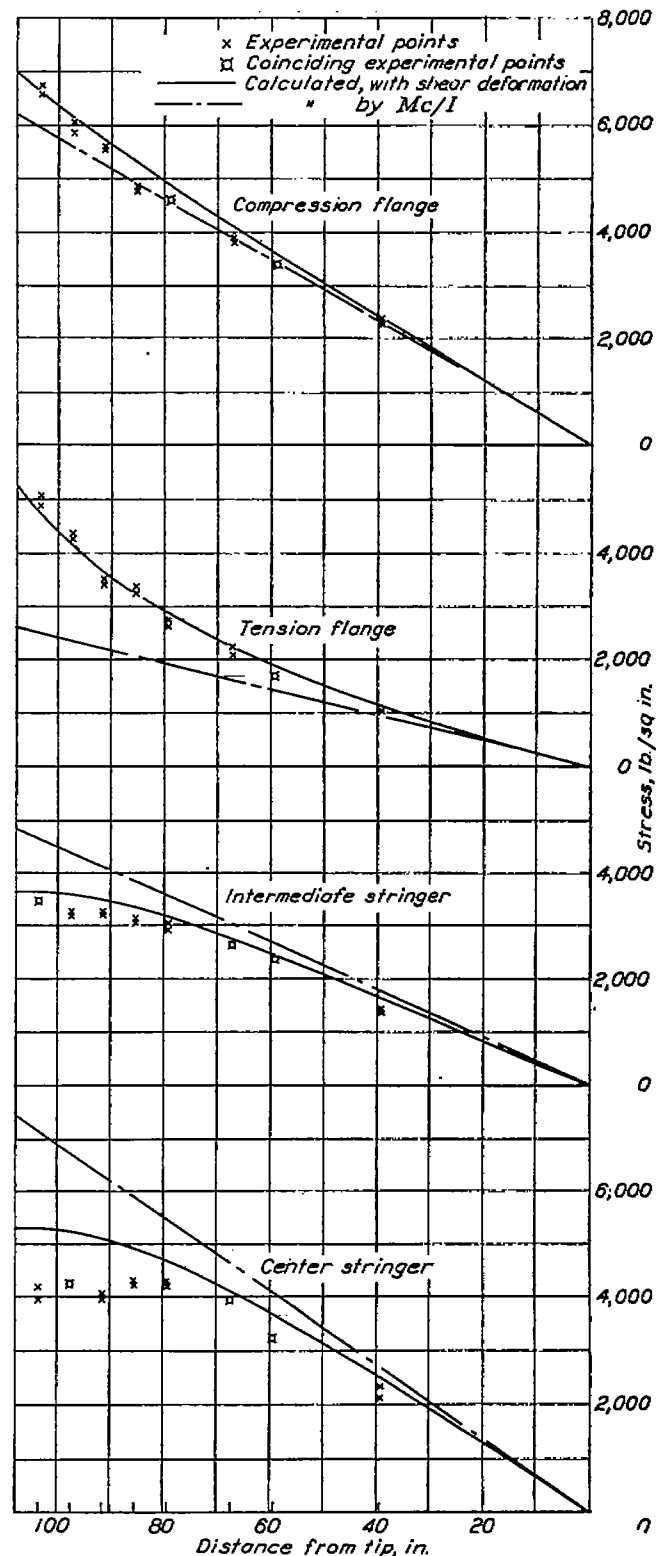


FIGURE 20.—Stresses in N. A. C. A. beam 3 for $P=250$ lb. $E=10.4 \times 10^4$.

poor for the beam with the thin cover (fig. 14 (a)) but is quite good for the beam with the thick cover (fig. 14 (b)).

For Schnadel's ship model, the agreement is fair at

some stations and very poor at others. Study of the test report shows that the accuracy of the test was, for a number of reasons, far below the accuracy of all other tests analyzed in the present paper. This conclusion is borne out by inspection of the results in figure 16. Note, for instance, at station 2 and particularly at station 3, that all experimental stresses are

beams under load shows that the spanwise variation in the condition of the sheet is indeed small; it should be borne in mind that relatively large variations in shear stiffness influence the stringer stresses but little, as shown in reference 1. The chordwise variation, however, is marked, the outer panels being buckled while the inner panels are not. This variation was taken

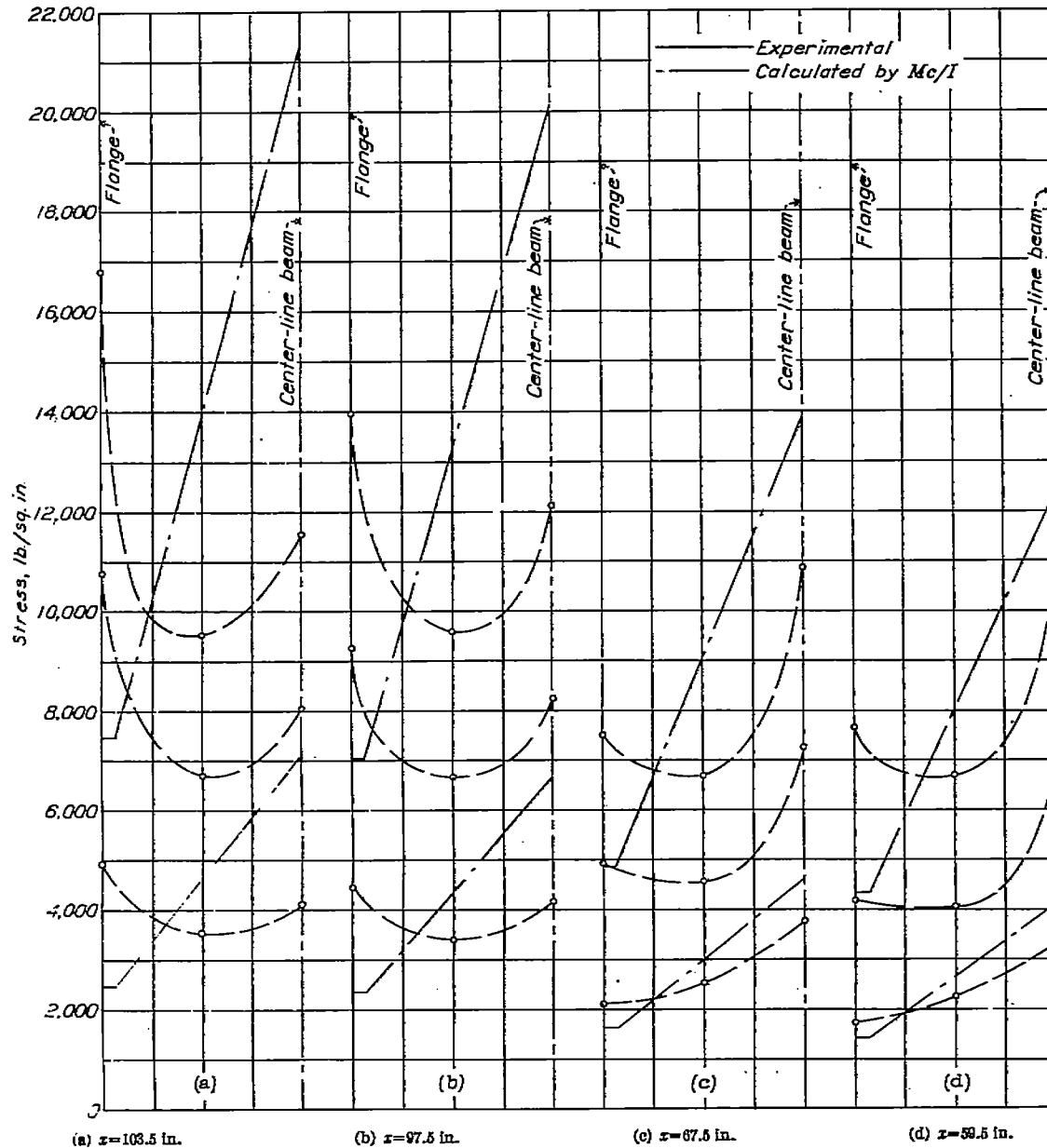


FIGURE 21.—Chordwise stress distribution in N. A. C. A. beam 3 at four stations for $P=250, 500,$ and 750 lb. Mc/I shown for $P=250$ and 750 pounds.

considerably higher than the calculated ones; hence the summation of the internal moments would be much larger than the external moment. The test was included in the analysis because it is the only available complete test on the limiting case where stringers and sheet are merged into a single unit, a plate.

In all beam analyses made for the present paper, over-all average values of effective shear stiffness were used. A glance at the photographs of the N. A. C. A.

into account approximately by using a weighted average value of G_s , and this procedure may be responsible for some of the discrepancies between test and calculation. Theoretically, it might be possible to take this variation into account more exactly, but there appears to be little justification to do so when the proposed simplified method of analysis is used. In practical design, large chordwise variations of shear stiffness should be avoided by using heavier skin near the flanges.

If the far-reaching simplifications involved in the theory are considered as well as the difficulties of strain-gage testing of sheet-metal structures, the agreement between experiments and analysis is, on the whole, fairly satisfactory. Although the analysis does not give a perfect picture of details, it does appear to give a substantially correct picture for the stresses most important in design work.

To persons unacquainted with strain-gage testing, the discrepancies between tests and calculations might appear to be rather large. It should be pointed out, however, that strain-gage tests of conventional types of structures, such as trusses and plate girders, frequently show discrepancies fully as large or larger.

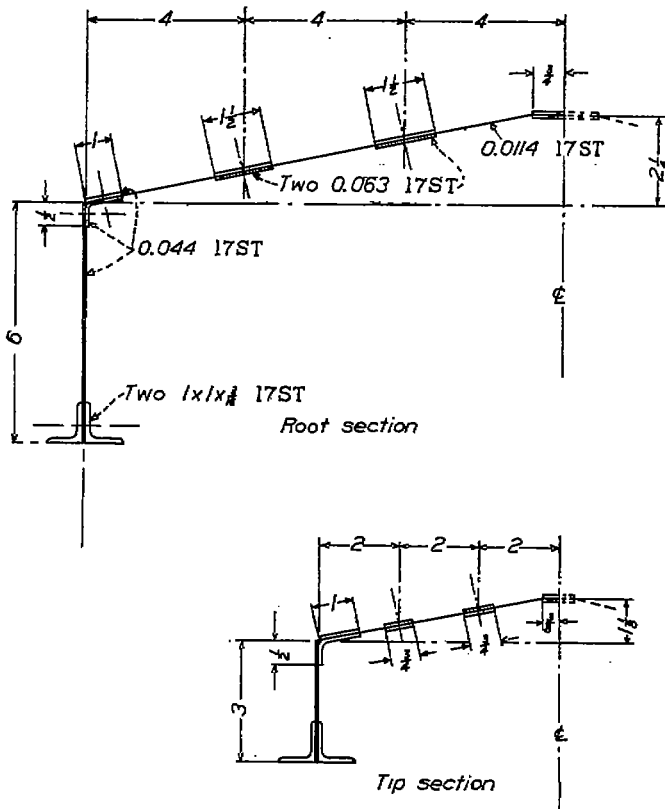


FIGURE 22.—Cross sections of N. A. C. A. beam 4.

COMPARISON BETWEEN PROPOSED METHOD OF ANALYSIS AND YOUNGER'S SOLUTION

The proposed method of analysis is based on the same simplified physical concepts as Younger's method (reference 1). Younger's solution is mathematically more rigorous, but it applies only to a beam of constant section with a cosine-wave bending moment. For practical shapes of bending-moment curves, it is necessary to superpose a number of cosine terms.

Comparisons for the case of a concentrated load applied at the tip show that the substitute-structure method of analysis gives flange stresses at the root that are as much as 15 percent higher than the stresses calculated by superposing four cosine terms. Judging by the magnitude of successive terms, four were considered a sufficient number to give the desired accuracy. The

stresses in the longitudinals given by the substitute-structure method are correspondingly lower than those given by Younger's formula. Comparison with experiments for two cases (figs. 9 and 12) shows that Younger's extended formula is in very much poorer agreement

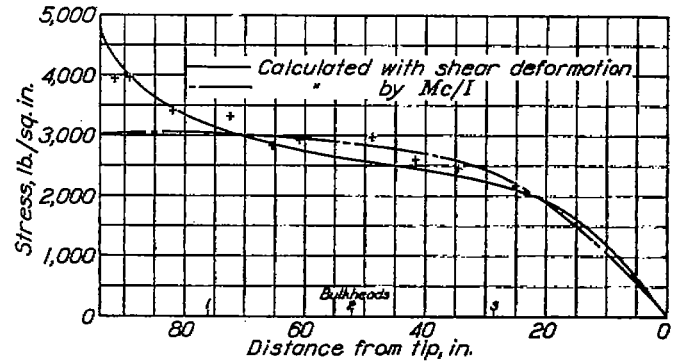


FIGURE 23.—Flange stresses in N. A. C. A. beam 4 at $P=250$ lb. $E=10.4 \times 10^6$.

with the experiments than the substitute-structure method. This fact is somewhat surprising, and the question arises as to what might be the possible reasons for the poor agreement.

If a diagonal-tension field forms on the sheet, the shear between flange and longitudinals will not be

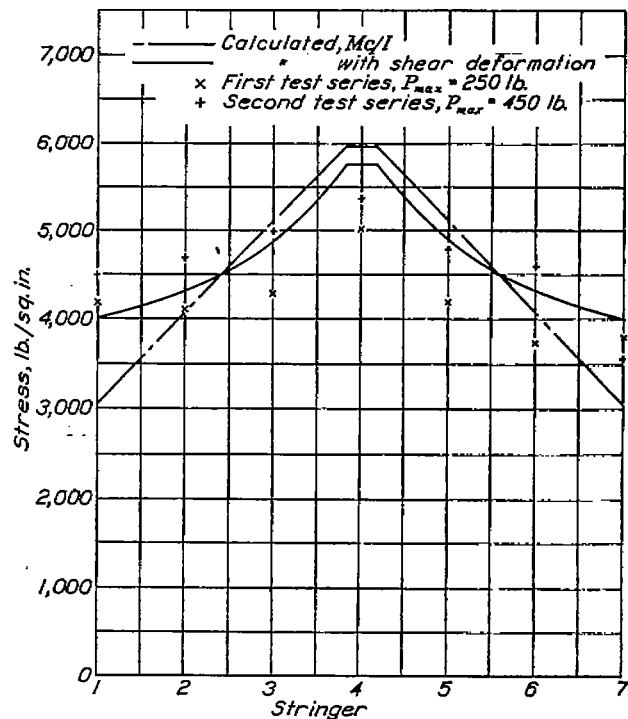


FIGURE 24.—Stresses at first station in N. A. C. A. beam 4.

transmitted at right angles to the axis of the beam but, theoretically, at 45° angles. The theory may therefore be expected to give reasonably accurate results only if the bending moment does not change too much over a spanwise distance equal to the width of the beam. Obviously, this condition is not fulfilled by the higher cosine terms after the first one, so that their physical significance may be seriously questioned.

The evidence presented by the axially loaded panel (fig. 9), which did not buckle appreciably at $P=1,000$ pounds, appears to indicate that even for a shear-resistant panel the superposition of cosine terms does not always yield a sufficiently close approximation to the physical facts. If this defect always exists, then any method based on the same fundamental physical concepts and relying on trigonometric series will be unreliable.

It might be mentioned in passing that the theoretical treatment given by Schnadel in reference 4 and in several other papers is of little interest for aeronautical structures, because it applies only to an isotropic plate where the shear stiffness is fixed by the theoretical relation

$$G = \frac{E}{2(1+\mu)}$$

The results therefore contain no provision to take into account reduced values of G , or plates stiffened by stringers.

THE INFLUENCE OF RIBS

Ribs or bulkheads influence the stresses in the beam cover in two ways. By virtue of their axial stiffness, they help to carry transverse stresses in the cover. This function is unimportant if the sheet does not buckle into a diagonal-tension field, but it is, of course, of paramount importance if a diagonal-tension field forms. Because the rib flanges have bending stiffness in the plane of the cover, they also tend to reduce the shear deformation. It was pointed out in reference 1 that this effect can be calculated for a single-stringer beam and it was stated that in practical cases the effect is very small. This conclusion, drawn from the calculations, has been confirmed by tests of N. A. C. A. beam 2. It should be noted, of course, that these remarks apply only if the basic requirement of very moderate camber is fulfilled.

N. A. C. A. beam 2 was tested first with all longitudinals sliding freely over the ribs and held against the ribs only by their own tension. A second strain survey was then made of the beam after connecting the longitudinals with the ribs by taper pins. The ribs were very heavy steel channels, as shown on the drawings and photographs, but their only effect was to smooth out a few minor irregularities in the stress-distribution plots. An extremely heavy tip rib was then added; this rib reduced the stress in the flange about 6 percent. Calculation indicated, however, that an equivalent amount of material used to thicken the skin would have resulted in increasing the skin thickness by about 500 percent over the entire span and would have reduced the stress in the flange by about 33 percent.

A brief inspection of figure 25 is sufficient to show why the rib is quite ineffective. Figure 25 (a) shows the tip rib acted upon by the longitudinal. In figure 25 (b) it was assumed that the material contained in the tip rib is spread out some distance along the span. It is obvious that this change results in a much stiffer cross beam.

All tests of N. A. C. A. beam 3 were made without connections between longitudinals and ribs. On N. A. C. A. beam 4, which had bulkheads of normal size, the longitudinals were riveted to the bulkhead flange.

THE EFFECTIVE SHEAR MODULUS

The effective shear modulus of a thin sheet framed by rigid edge members is equal to the shear modulus of the material as long as the shear stress is lower than the critical or buckling stress. If the stress is increased beyond this value, diagonal-tension folds begin to form and grow. The effective shear modulus gradually decreases, approaching asymptotically the value $G_e = \frac{1}{2}G$. The nature of this transition was investigated experimentally by Lahde and Wagner (reference 5).

In practical structures, the edge members are not rigid; they have a finite axial stiffness and a finite bending stiffness. The influence of these stiffnesses has been treated analytically by Wagner in his original theory for the case of a fully developed diagonal-tension field. The influence of edge members with finite stiffness on the characteristics of a thin sheet in the transi-

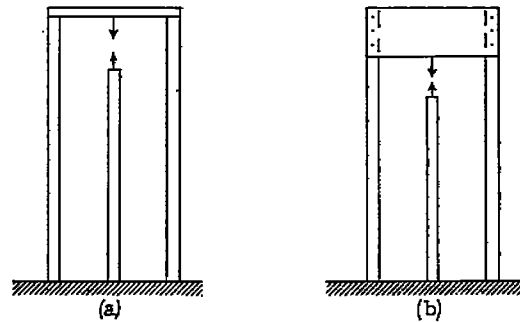


FIGURE 25.

tion zone between shear-resistant sheet and diagonal-tension field has not been investigated to date. Atkin offers a method of estimating the characteristics of a diagonal-tension beam by making tests on square panels (reference 6). Although this idea is fundamentally sound, Atkin's analysis is open to a serious objection. He claims that the deflection δ of a test panel can always be represented as a straight-line function of the load P , and he sets

$$\delta = kP$$

which means, in effect, that Atkin's method takes into account only the finite stiffness of the edge members. It disregards the gradual transition from $G_e = G$ to $G_e = \frac{1}{2}G$ in a rigidly framed sheet. In many practical cases, where the critical stress is not exceeded more than three or four times, the second factor is probably far more important than the first.

The tests described in references 2 and 3 were evaluated by their authors to give values of effective shear stiffness. These analyses have been questioned in a later paper (reference 7), chiefly because the values obtained were much lower than the theoretical values for the pure diagonal-tension field with rigid edge members.

A critical examination shows that in all these analyses the shear stiffness has been obtained by taking the differences of slopes of two experimental curves. This method is extremely sensitive to slight experimental errors. Unfortunately, experimental errors in strain-gage tests of sheet-metal structures are quite large, and the stresses are, furthermore, quite insensitive to changes in shear stiffness. The results obtained by such a slope method are therefore very questionable, and in some cases it is possible to change the calculated values of the shearing stiffness several hundred percent by

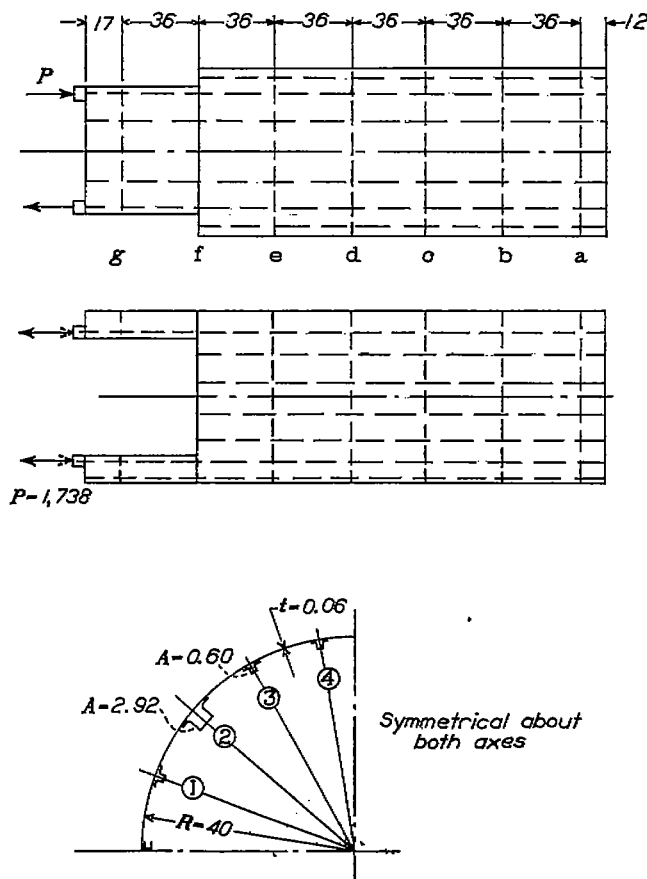


FIGURE 26.—Test fuselage (data from reference 10). Dimensions are in cm and loads in kg.

varying, for instance, the effective width within its possible limits.

In view of these circumstances, it appears more advisable to analyze the tests in such a manner that over-all average values for the shear stiffness are obtained by utilizing the ordinates of experimental curves instead of the slopes of these curves. The procedure would be to calculate the stresses under several assumptions for the shear stiffness and to find the stress curve that gives the best agreement with the test results. Several examples of such a procedure are given in reference 1.

The high-load tests of N. A. C. A. beam 3 were analyzed in a similar manner. Unfortunately, the limited number of strain gages necessitated repeat load-

ings; during these repeat tests, changes occurred in parts of the beam that prevented a definite analysis. It was estimated that, at $P=900$ pounds, the effective shear modulus was $G_e=0.5G$, but no definite estimate could be made for higher loads. The trouble may have been partly that the flange was no longer obeying Hooke's law at the gage station, the stress being over 30,000 pounds per square inch.

It should be noted that the effective modulus was well below the theoretical value $G_e=\frac{5}{8}G$ for rigid edge members, in spite of the fact that the edge members were much stiffer than they would be in actual construction and that tension was superimposed on the shear in the skin.

The opinion is occasionally heard that the shear modulus of corrugated sheet is appreciably less than that of flat sheet. There appears to be no published information to support such an opinion. The analysis of torque tests of box beams with corrugated covers (reference 8) leads to the conclusion that up to shear stresses of around 3,000 pounds per square inch the shear modulus of corrugated sheet is equal to the modulus of the material. Small deviations of 5 to 10 percent, which occur in such tests, can probably be attributed to inefficiency of the joints in the built-up boxes because they have been found in practically all torque tests. Ebner, who has an exceptionally broad background of experience in tested stressed-skin structures, states in reference 9 that the shear stiffness of corrugated sheet remains unchanged up to the point of failure. It is necessary, of course, to make proper allowance for the difference between developed width and projected width of a corrugated panel when computing shear deformations.

APPLICATION OF THEORY TO FUSELAGES

The theory in this paper was developed for the express purpose of furnishing means for analyzing wing beams or other beams with very moderate camber. It is of interest, of course, to gain some idea of how well the theory applies to beams with large camber, such as fuselages. A fuselage test that came to the attention of the author after the investigation was finished will therefore be included.

The details of the test may be found in reference 10. The most important data are given in figure 26. The shell represents a fuselage with symmetrical cut-outs, and the bending moment is introduced in the form of concentrated forces at the longerons. Between frame a and the end, the shell was fixed to a test jig by a heavy steel ring.

The part of the shell between the longerons and the neutral axis was considered as "shear web" and the remainder as "cover." The analysis was made by formula (A-16). Local corrections to the computed stresses were made between frames e and g, because the sheet thickness was 0.08 centimeter between e and

f, and 0.10 centimeter between f and g resulting, together with the cut-out, in some changes in effective areas in this region.

The only variation from the standard procedure outlined in this paper was the use of a somewhat more rational method of determining c_s than simply assuming $c_s = \frac{1}{2}c$. The substitute camber was determined by the condition.

$$\left(c_s + \frac{1}{2}h_w\right)^2 A_L = I_L$$

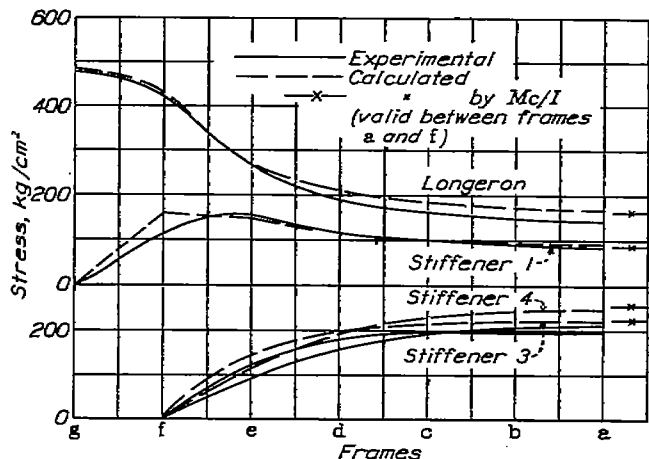


FIGURE 27.—Experimental and calculated stress distribution in fuselage with symmetrical cut-outs (experimental data from reference 10).

That is, if the longitudinals are concentrated at the z location defined by c_s , the moment of inertia must be the same as in the actual section.

Figure 27 shows the experimental and the calculated results.

CONCLUDING REMARKS

Large shear deformations are probably always accompanied by loss of structural efficiency; efficient design therefore calls for utilization of all available means for reducing the shear deformation. In a combination consisting of skin stiffened by individual stringers, the stringers furnish no contribution to the shear stiffness. In a combination of flat skin with corrugated skin, however, all the material carries longitudinal stresses as well as shearing stresses; such a

combination probably represents, therefore, a close approach to the best possible efficiency from considerations of uniform stress distribution. It must be remembered, too, that the shear stiffness of flat sheet is very adversely affected if it is thin enough to buckle into diagonal-tension folds, a condition that does not develop in corrugated sheet.

For sheet with individual stringers, experimental studies on individual panels have usually led to the conclusion that the best efficiency is obtained by making the skin as thin as possible, consistent with practical considerations. If the shear deformation in the actual structure is taken into account, it becomes evident that this conclusion will often require serious modification. It might be worth while in some cases to investigate the effect of thickening the skin near the wing tip, where the shear deformations are largest and therefore easiest to decrease. It might be pointed out that, once an adequate tip rib is provided, shear deformation can be reduced more efficiently by increasing the skin thickness, especially near the tip, than by attempting to increase the (horizontal) bending stiffness of the tip rib.

A final word of warning should be given. A method of stress analysis such as the method described in this paper deals only with the stress distribution before failure occurs. If the maximum stress for a given load is varied by changing the design of the structure, then the failing stresses may change, too, so that the maximum stress is not the sole criterion for the efficiency of the structure. For example, if the skin is made very heavy with relation to the stringers, then buckling of the skin may induce premature failure of the stringers. Thus far, no mathematical analysis of this problem has been published; test results must be used. The subject of allowable stresses is beyond the scope of this paper, but is mentioned herein as a warning against drawing hasty conclusions.

LANGLEY MEMORIAL AERONAUTICAL LABORATORY,
NATIONAL ADVISORY COMMITTEE FOR AERONAUTICS,
LANGLEY FIELD, VA., April 20, 1938.

APPENDIX A

LIST OF SYMBOLS

A , cross-sectional area (sq. in.).
 E , Young's modulus (lb./sq. in.).
 F , internal force (lb.).
 G , shear modulus (lb./sq. in.).
 I , geometric moment of inertia.
 K , constant.
 L , length of panel or beam (in.).
 M , bending moment (in.-lb.).
 P , external load (lb.).
 S , shear force (lb.).
 b , half-width of beam or panel (in.).
 c , camber of cover (in.).
 h , depth of beam (in.).
 t , thickness of cover sheet (in.).
 w , running load (lb./in.).
 x , distance along center line.
 y , distance from center line.
 z , distance from centroidal axis of cross section.

486

σ , direct (normal) stress (lb./sq. in.).
 τ , shear stress (lb./sq. in.).
*, denotes condition where actual and auxiliary stresses are superposed.
Subscripts have the following significance:
 A , auxiliary.
 C , cover sheet.
 CL , center line.
 F , flange.
 L , longitudinal.
 P , theoretical values assuming that plane sections remain plane.
 S , substitute.
 T , total.
 U , uniform.
 W , shear web.
 a , applied.
 e , effective.
 0 , root section.

APPENDIX B

ANALYTICAL SOLUTIONS FOR STRUCTURES WITH A SINGLE LONGITUDINAL

GENERAL REMARKS

The sign conventions of reference 1 are retained. Stresses in stringers are positive when tensile. Shear stresses in the cover sheet are positive when caused by positive stresses in the flange F . Shear stresses in the shear web are positive when causing positive stresses in the flange F .

The figures show, first, the half structures and, second, the two possible cases of making symmetrical structures out of these half structures. The formulas should be applied only to such symmetrical structures. Theoretically, the formulas also apply to the half structures if the forces T are applied at the stiff transverse member at the tip. This procedure would involve the assumption that the stringers were infinitely stiff in bending; it is therefore believed that the application of the formulas to the half structures might easily lead to very serious errors.

Some of the formulas have already been given in reference 1. They are repeated here for convenience and are written in a slightly different form to bring out more clearly the correction factor that must be applied to the

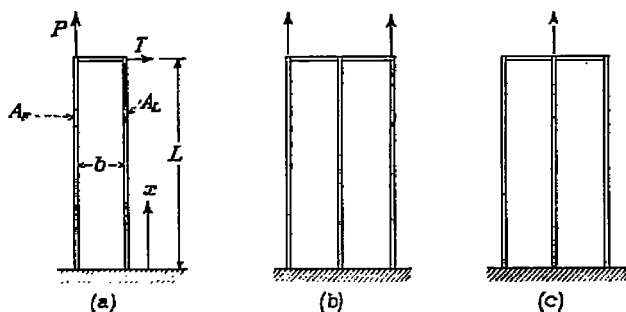


FIGURE 28.

ordinary bending theory in order to take shear deformation into account. When the shear stiffness approaches infinity, this correction factor approaches zero.

I—THE AXIALLY LOADED PANEL

(a) The longitudinal built in at the root (fig. 28).—For the case of an axially loaded panel with the longi-

tudinal built in at the root, the following formulas are obtained:

Let

$$K^2 = \frac{G_s t}{E b} \left(\frac{1}{A_F} + \frac{1}{A_L} \right) \quad (\text{A-1})$$

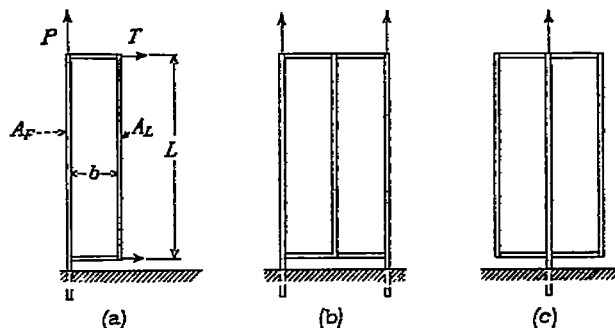


FIGURE 29.

and

$$A_T = A_F + A_L$$

Then

$$\tau = \frac{P}{A_F} \frac{G_s}{E b K} \frac{\sinh Kx}{\cosh KL} \quad (\text{A-2})$$

$$\sigma_F = \frac{P}{A_T} \left(1 + \frac{A_L}{A_F} \frac{\cosh Kx}{\cosh KL} \right) \quad (\text{A-3})$$

$$\sigma_L = \frac{P}{A_T} \left(1 - \frac{\cosh Kx}{\cosh KL} \right) \quad (\text{A-4})$$

(b) The longitudinal not built in at the root (fig. 29).—The easiest way to treat the case of the longitudinal not built in at the root is to take advantage of the symmetry of the structure. When the origin is taken at the middle of the length L , this case is reduced to case I (a).

II—THE BEAM WITH FLAT COVER

The formulas for the beam with flat cover apply to two cases: beams in which the depth h is constant along the span, if a concentrated load P is applied at the tip; and beams in which the depth h tapers linearly to zero at the tip, if the loading w per foot run is uniform along the span. In the case of uniform loading, $wL/2h_0$ is substituted for P/h in the formulas for shear stress.

(a) The longitudinal built in at the root (fig. 30).—

$$\tau = \frac{P}{th \left(1 + \frac{A_F}{A_L}\right)} \left(1 - \frac{\cosh Kx}{\cosh KL}\right) \quad (A-5)$$

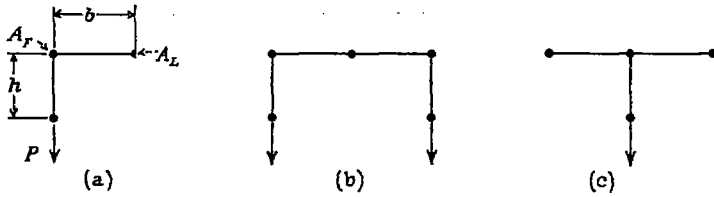


FIGURE 30.

$$\sigma_F = \frac{M_x}{h_x A_T} \left(1 + \frac{A_L}{A_F} \frac{\sinh Kx}{Kx \cosh KL}\right) \quad (A-6)$$

$$\sigma_L = \frac{M_x}{h_x A_T} \left(1 - \frac{\sinh Kx}{Kx \cosh KL}\right) \quad (A-7)$$

where K has the same meaning as in (A-1).

(b) The longitudinal not built in at the root.—The case of a beam with flat cover and the longitudinal not built in at the root is of interest as a limiting case for wings where the skin is not continuous, for example, at the wing-fuselage joint.

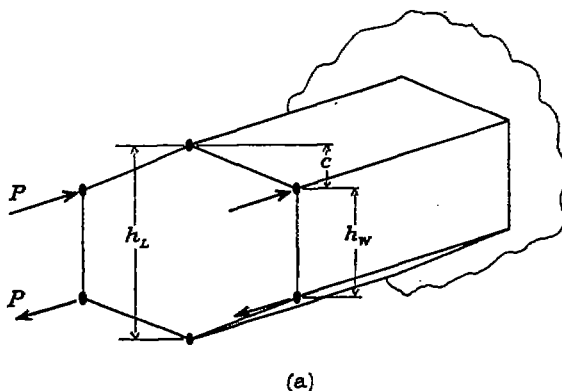
$$\tau = \frac{P A_L}{t h A_T} \left(1 - \frac{KL \cosh Kx}{\sinh KL}\right) \quad (A-8)$$

$$\sigma_F = \frac{M_x}{h_x A_T} \left(1 + \frac{A_L}{A_F} \frac{L \sinh Kx}{x \sinh KL}\right) \quad (A-9)$$

$$\sigma_L = \frac{M_x}{h_x A_T} \left(1 - \frac{L \sinh Kx}{x \sinh KL}\right) \quad (A-10)$$

III—THE BEAM WITH CAMBERED COVER

As in the case of the beam with flat cover, the formulas for the beam with cambered cover are valid for two cases: for a concentrated load P applied at the tip, if h and c are constant; and for a uniformly distributed load w per foot run, if h and c taper linearly to zero at the tip. For the tapered beam, $wL/2$ is substituted for P , and z_L and I are taken at the root station in the formula for shear stress only.



(a) The longitudinal built in at the root (fig. 31).—

$$\tau = \frac{P z_L A_L}{t I} \left(1 - \frac{\cosh Kx}{\cosh KL}\right) \quad (A-11)$$

$$\sigma_F = \frac{M z_F}{I} \left[1 + \frac{z_L A_L}{z_F A_F} \left(1 + \frac{c}{h_w}\right) \frac{\sinh Kx}{Kx \cosh KL}\right] \quad (A-12)$$

$$\sigma_L = \frac{M z_L}{I} \left(1 - \frac{\sinh Kx}{Kx \cosh KL}\right) \quad (A-13)$$

In these equations, I is the geometric moment of inertia, z_L is the distance of the longitudinal from the centroidal axis, and K is defined by

$$K^2 = \frac{G_c t}{E b'} \left(\frac{1 + \frac{c}{h}}{A_F} + \frac{1}{A_L}\right) \quad (A-14)$$

(b) The longitudinal not built in at the root.—The formulas for the case of the longitudinal not built in at the root may be obtained by changing the factors in parentheses in analogy with cases II (a) and II (b).

IV—THE BEAM WITH CAMBERED COVER IN "PURE BENDING"

The formulas for the case shown in figure 32 (a) are:

$$\tau = \frac{P G_c \sinh Kx}{E b' K \cosh KL} \left(\frac{1}{A_F} + \frac{c h_w}{I}\right) \quad (A-15)$$

$$\sigma_F = \frac{P h_w^2}{2 I} \left[1 + \frac{A_L}{A_F} \left(\frac{h_L}{h_w}\right)^2 \frac{\cosh Kx}{\cosh KL}\right] \quad (A-16)$$

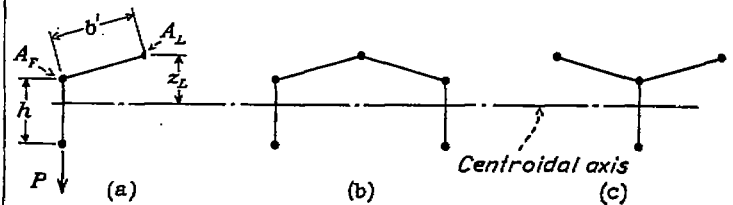


FIGURE 31.

where K is defined by

$$K^2 = \frac{G_c t}{E b'} \left(\frac{1 + \frac{2c}{h_w}}{A_F} + \frac{1}{A_L}\right) \quad (A-17)$$

FIGURE 32.

It should be noted that there is shear in the shear web, because the shear in the cover sheet has a component in the z direction. For this reason, the cambered cover cannot be used alone as an axially loaded panel unless provisions are made to absorb this lateral force, for instance, by making the panel symmetrical as in figure 32 (b).

REFERENCES

1. Kuhn, Paul: Stress Analysis of Beams with Shear Deformation of the Flanges. T. R. No. 608, N. A. C. A., 1937.
2. White, Roland J., and Antz, Hans M.: Tests on the Stress Distribution in Reinforced Panels. Jour. Aero. Sci., vol. 3, no. 6, April 1936, pp. 209-212.
3. Lovett, B. B. C., and Rodee, W. F.: Transfer of Stress from Main Beams to Intermediate Stiffeners in Metal Sheet Covered Box Beams. Jour. Aero. Sci., vol. 3, no. 12, Oct. 1936, pp. 426-430.
4. Schnadel, Georg: Die Spannungsverteilung in den Flanschen dünnwandiger Kastenträger. Jahrbuch der Schiffbau-technischen Gesellschaft, 1926, S. 207-291.
5. Lahde, R., and Wagner, H.: Tests for the Determination of the Stress Condition in Tension Fields. T. M. No. 809, N. A. C. A., 1936.
6. Atkin, E. H.: Stiffness in Stressed Skins. A Method of Determining the Shear Rigidity from Experimental Data on Small Panels. Aircraft Engineering, vol. VIII, no. 90, Aug. 1936, pp. 213-217, 220.
7. Lin, Tung-Hua: On the Transfer of Stress in Metal Sheet Covered Beams. Jour. Aero. Sci., vol. 4, no. 12, Oct. 1937, pp. 510-511.
8. Kuhn, Paul: The Initial Torsional Stiffness of Shells with Interior Webs. T. N. No. 542, N. A. C. A., 1935.
9. Ebner, H.: Zur Festigkeit von Schalen- und Rohrholmflügeln. Jahrbuch der Deutsche Luftfahrtforschung, 1937, S. I 430 - I 441. (Also published in Luftfahrtforschung, Bd. 14, Lfg. 4/5, 30. April 1937, S. 179-190.)
10. Schapitz, E., and Krümling, G.: Belastungsversuche mit einer versteiften Kreiszyinderschale bei Krafteinleitung an einzelnen Punkten. Luftfahrtforschung, Bd. 14, Lfg. 12, 20. Dez. 1937, S. 593-606.